frontiers in Earth Science

ORIGINAL RESEARCH
published: 24 March 2022
doi: 10.3389/feart.2022.865534

Fracture Characteristics and its Role in Bedrock Reservoirs in the Kunbei Fault Terrace Belt of Qaidam Basin, China

Zhaosheng Wang[1], Hui Xiang[2], Libin Wang[3], Lin Xie[4], Zhenguo Zhang[1,5], Lianfeng Gao[1], Zhifeng Yan[1] and Fuling Li[1]*

[1]College of Mining Engineering, Liaoning Technical University, Fuxin, China, [2]Zhundong Oil Production Plant, Xinjiang Oilfield Company, Petro China, Fukang, China, [3]Research Institute of Petroleum Exploration and Development, Petro China, Beijing, China, [4]Research Institute of Petroleum Exploration and Development, Qinghai Oilfield Company, Petro China, Dunhuang, China, [5]College of Mining Engineering, North China University of Science and Technology, Tangshan, China

Fracture characteristics at bedrock reservoirs in the Kunbei fault terrace belt in the southwest of Qaidam Basin, China, are investigated based on cores, thin sections, formation microscanner imaging, and production data. Results show that the weathered unit at the top of bedrocks is not an effective reservoir because of extremely low porosity. A semi-weathered unit is a potential reservoir, where formation water migrating along early effective fractures could form dissolution fractures and pores as primary storage space, and fractures can also act as seepage channels. Four fracture types can be identified from bedrock reservoirs, e.g., structural ones, diagenetic ones, weathering ones, and dissolution ones, while shear fractures related to faults are the most important ones. Fracture types and characteristics are different in granite and slate, e.g., high fracture density results in intensive dissolution in granite. Fracture density is closely related to tectonic stress. The bedrock reservoirs near fault zones and semi-weathered units are potential oil and gas exploration targets in the Kunbei fault terrace belt. Effective fractures govern dissolution behaviors as well as dominant seepage directions, which play a significant role in the development of bedrock reservoirs.

Keywords: fractures, bedrock reservoirs, *in-situ* stress, fracture identification, distribution characteristics

OPEN ACCESS

Edited by:
Kouqi Liu,
Central Michigan University,
United States

Reviewed by:
Jinxiong Shi,
Yangtze University, China
Wenya Lyu,
China University of Petroleum, China

****Correspondence:***
Zhaosheng Wang
zhaoshengw@126.com

Specialty section:
This article was submitted to Structural Geology and Tectonics, a section of the journal Frontiers in Earth Science

Received: *30 January 2022*
Accepted: *25 February 2022*
Published: *24 March 2022*

Citation:
Wang Z, Xiang H, Wang L, Xie L, Zhang Z, Gao L, Yan Z and Li F (2022) Fracture Characteristics and its Role in Bedrock Reservoirs in the Kunbei Fault Terrace Belt of Qaidam Basin, China. Front. Earth Sci. 10:865534. doi: 10.3389/feart.2022.865534

INTRODUCTION

Bedrocks are defined as all rocks forming a basin basement, which are commonly buried under sedimentary rocks (Miriam et al., 2010). With increasing oil and gas exploration practices, bedrock reservoirs (including metamorphic and plutonic rocks) have become potential unconventional oil and gas exploration targets, which increasingly attracts the attention of petroleum geologists and engineers (Tamagawa and David, 2008; Tong et al., 2017; Wang J. Q. et al., 2021). Hydrocarbon in bedrock reservoirs was primarily sourced from upper sedimentary sequences *via* unconformities or faults (Bagriy and Griga, 2015), which was characterized as a "new source to old reservoir" (Ma et al., 2006). The bedrocks can be favorable reservoirs as they are adjacent to hydrocarbon generation centers, high-quality reservoir-cap assemblages, and conduit systems (Zhu et al., 2020). The storage space in bedrock reservoirs includes fractures associated with tectonism, weathering, and dissolution, as well as dissolution pores (Shanley and Cluff, 2015; Zhang et al., 2021), whose production behavior varies greatly with fracture

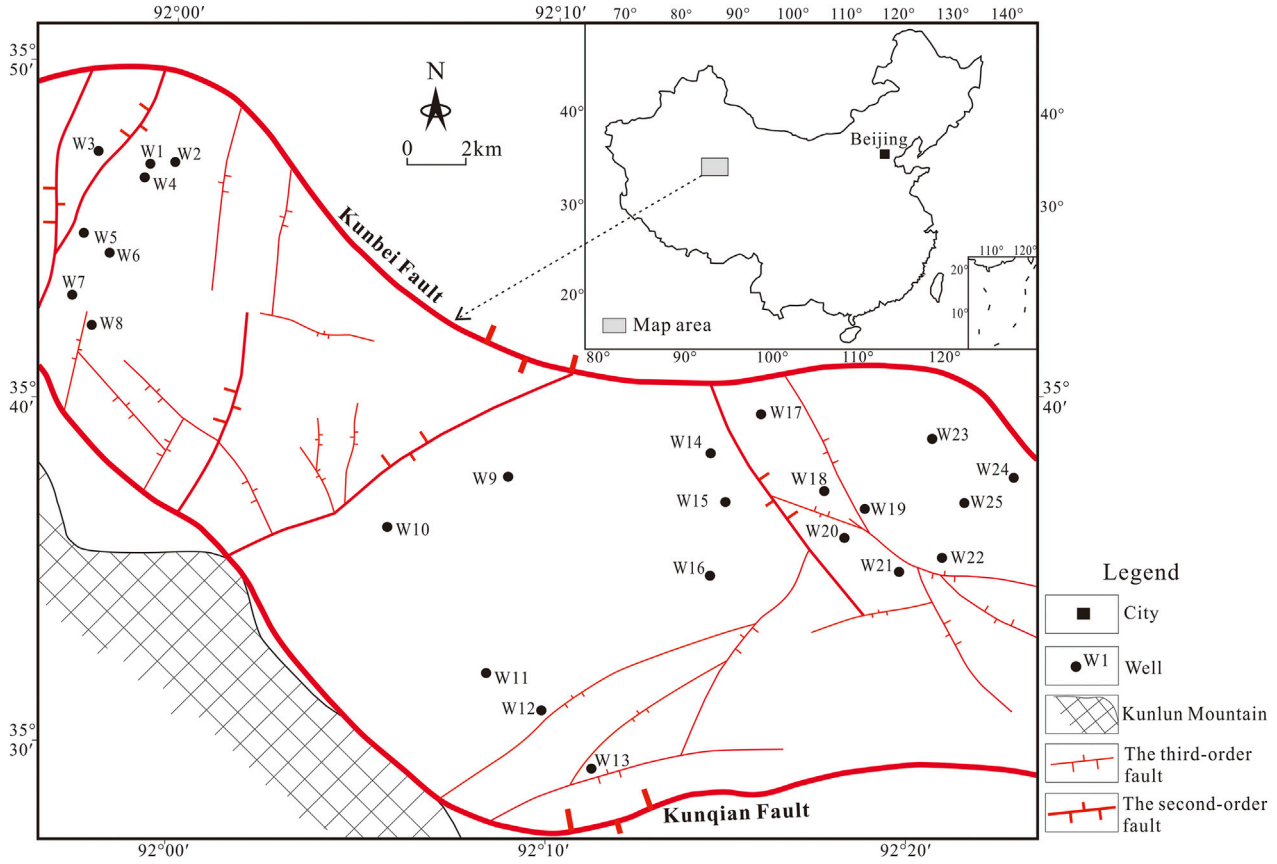

FIGURE 1 | Structure location of the study area.

density, connectivity, and distribution (Wu et al., 2012). Variations in mineral compositions and rock structures give rise to different weathering resistance and dissolubility of bedrocks, resulting in strong heterogeneity in fracture growth (Wishart et al., 2008; Liu, 2012). Consequently, bedrock reservoirs are commonly characterized by high initial production, but rapid decline with short or no stable period. Therefore, understanding fracture characteristics and their primary controllers is critical for the efficient exploration and development of bedrock reservoirs.

In this paper, taking bedrock reservoirs in the Kunbei fault terrace belt in southwestern Qaidam Basin, China, as an example, we systematically investigated fracture characteristics in bedrock reservoirs and their role in hydrocarbon accumulation and reservoir development through integrating geology, imaging log, and experiment and production data.

GEOLOGICAL SETTING

Structure

Kunbei fault terrace belt in the southwest of Qaidam Basin in China is an inherited uplift developing on Paleozoic metamorphic rocks and Hercynian granite (Liu et al., 2015). The study area is a NW-NWW extending transpressional structural system controlled by basin-range coupling and tectonic evolution, especially the NS-trending tectonic dynamics during Himalayan movement (Fu et al., 2010) (**Figure 1**) NW-trending faults control primary structural trends as well as alternated sags and uplifts in the Kunbei fault terrace belt, where NS-trending secondary faults modified local structures. Diverse traps were developed in the Kunbei fault terrace belt, including faulted noses, faulted blocks, and faulted anticlines. (Chen et al., 2010).

Oil Source

Oil source correlation shows that oil and gas in the Kunbei fault terrace belt are mainly derived from the Qiekelike Sag in the northeast (Liu et al., 2008; Wu et al., 2014), where E_3^2 and N_1 source rocks are developed with an area over 2000 km^2. The average organic carbon content (TOC) of E_3^2 source rocks is 0.85%. Ro values are about 0.5–1.1%, indicating that source rocks are at the hydrocarbon generation peak (Chen et al., 2012; Gao et al., 2014). They are high-quality source rocks for bedrock reservoirs in the Kunbei fault terrace belt.

Reservoirs

The eastern Kunbei fault terrace belt is dominated by a granite basement, while the western has a compound basement

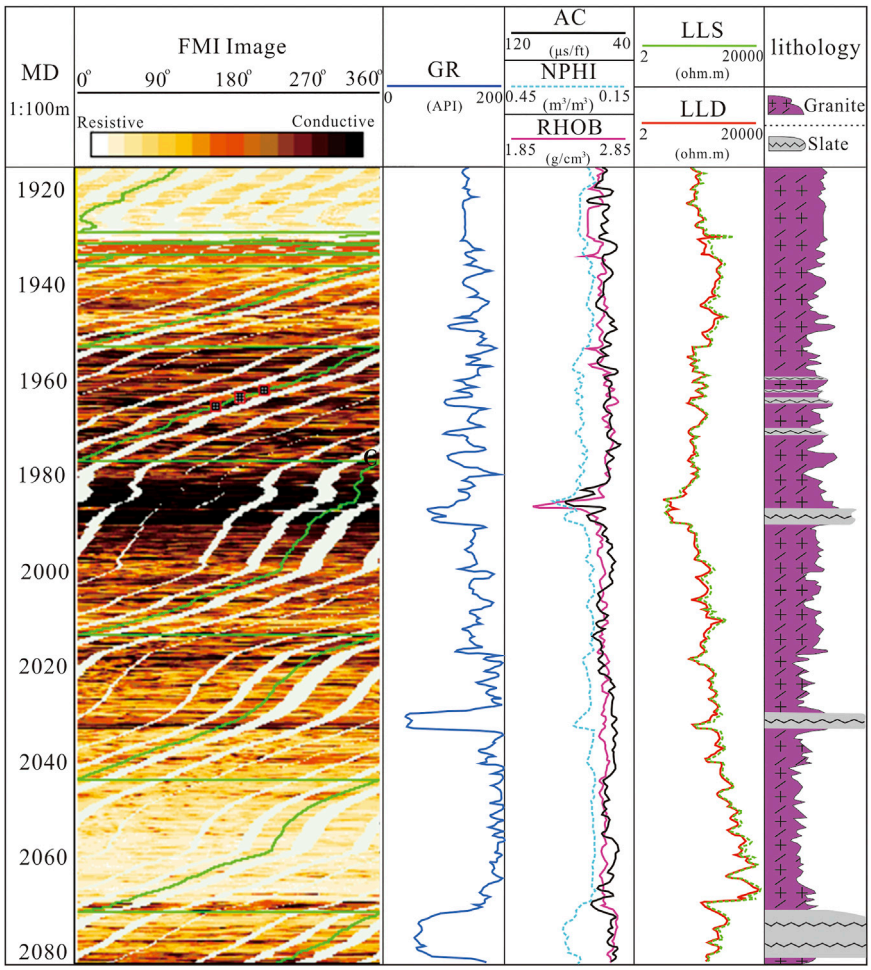

FIGURE 2 | FMI image and logging response of bedrock sections from the well W5. See **Figure 1** for well W5 location.

dominated by metamorphic rocks and granite, with a small amount of siliceous rocks and metasandstone (Li et al., 2011). Granite is a typical plutonic intrusive rock that is dominated by potassium feldspar, plagioclase, quartz, and biotite, with amphibole and muscovite of secondary importance. It is surrounded by metamorphic rocks, mainly slate with a small amount of metasandstone. The slate is primarily composed of sericite, with a small amount of feldspar, quartz, and carbonate minerals, such as ferrocalcite and ferrodolomite. (Liu et al., 2015). The storage space is dual medium consisting of pores and fractures, where matrix porosity is 1.5–4.5%, with an average value of 2.8%, and permeability varies between 0.02×10^{-3} μm^2 and 5.5×10^{-3} μm^2, with an average value of 0.6×10^{-3} μm^2.

Production Performance

The pilot production of bedrock reservoirs in the Kunbei fault terrace belt shows that both granite and slate have good production performance, which varies greatly among different structures, e.g., wells at the structure edge have low production and low efficiency. Wells at structure highs, however, have large reservoir thickness and good oil shows, whose initial production is high but decreases rapidly after water injection. The bedrock reservoirs in the Kunbei fault terrace belt have clear oil-water contacts, where no stable interlayer is developed between the bedrock and the E_3^1 sandstone at the top. It is a typical structural reservoir controlled by bottom water with unified oil-water system.

MATERIALS AND METHODS

Fractures are identified and described based on formation microscanner imaging log(FMI) data from seven wells with total length of 539.1 m, coring data from 20 wells with length of 109.9 m, and production data from 25 wells.

Lithology Recognition

The boundary between bedrocks and sedimentary rocks in the study area can be easily identified with sharp change in gamma-ray log and resistivity log. Granite and slate can be distinguished from FMI images, e.g., the former appears as block in FMI images, while the latter is lamina. Meanwhile, the gamma-ray curve varies

TABLE 1 | Fracture patterns on FMI images.

Fracture Types		Features
Natural fractures	Small Faults	Single Dark Sine Curve, with Aperture of Hundreds of Microns
	Effective fractures	Multiple dark sine curves (low-resistivity) in groups, various occurrence, network-like, with aperture of tens to hundreds of microns
	Half-filled fractures	Sine curves with alternated light and dark, with aperture of tens to hundreds of microns
	Completely-filled fractures	Bright sine curves (high-resistivity), with aperture of tens to hundreds of microns
Induced fractures	Fractures associated with stress-releasing	Incomplete sine curves, in en echelon arrangement, identical occurrence
	Fractures associated with heavy mud	Dark double curves, in symmetrical pattern, with length of centimeters to meters

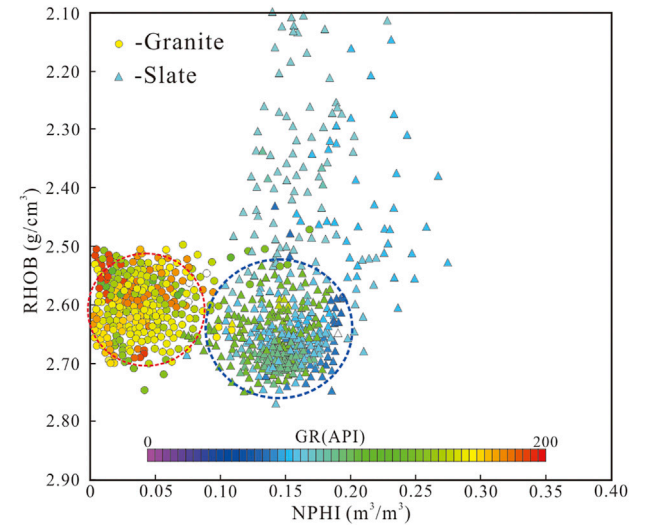

FIGURE 3 | Cross plot of RHOB-NPHI from FMI logging data (N = 694).

significantly at the boundary between granite and slate (**Figure 2**), e.g., granite is characterized by high gamma-ray (80–190 API). High-density granite has obvious low neutron porosity hydrogen index (NPHI) (< 0.10) and high litho-density (RHOB) (2.50–2.70 g/m^3) (**Figure 3**). Slate has an obvious low gamma-ray (40–80 API) and high NPHI (0.07–0.22) and RHOB (2.55–2.75 g/m^3) (**Figure 3**).

Fracture Identification and Quantitative Evaluation

Fractures providing reservoir space and/or seepage channels are defined as effective (Zeng et al., 2010). FMI can provide visualized information about locations and features of natural fractures, induced fractures, and small faults. Natural fractures can be represented by sine curves on FMI images, while effective fractures are dark sine curves due to good conductivity after being filled by drilling fluid (Huang, et al., 2006). Mutual cutting can be observed among multiple groups of fractures, which are ineffective after being completely filled with minerals (e.g., calcite or quartz). Poor conductivity leads to bright sine curves on FMI images (Qu et al., 2016). The characteristics of different types of fracture on FMI images are shown in **Table 1** (Jan et al., 1995).

Fracture density is often expressed by fracture numbers per unit length, 1/m or 1/ft. Fracture aperture and porosity from FMI are deduced as the following **Equations 1**, **2** (Luthi and Souhaite, 1990):

$$W = CAR_{mf}^{b} R_{xo}^{1-b} \tag{1}$$

Where W is fracture aperture (mm), C and b are coverage ratios of FMI, A is the increased current due to fractures (mA), R_{mf} is resistivity of mud filtrate (Ω▪ m), and R_{xo} is resistivity of detected zone (Ω▪ m).

$$\varphi_f = \frac{1}{2\pi RLC} \sum_{i=1}^{n} L_i W_i \tag{2}$$

Where Φ_f is fracture porosity (%), R is well radius (meter), L is length of statistical interval (meter), L_i is fracture length in image (meter), and W_i is fracture aperture (millimeter).

Considerable data shows that fracture permeability is positively correlated with porosity and aperture (Hoffman and Narr, 2012), hence fracture permeability can be determined by the following (Niu et al., 2010):

$$K_f = eW^m \varphi_f \tag{3}$$

Where K_f is fracture permeability ($\times 10^{-3}$ μm^2) and e is empirical coefficient, m is 1.5–2.0.

RESULTS

Bedrocks in the Kunbei fault terrace belt can be divided into three units from top to bottom: weathered unit dominated by clay, semi-weathered unit, and fresh unit. The weathered unit is characterized by small thickness (0–2.5 m, average: 1.9 m) and extremely low porosity, which is not regarded as a high-quality reservoir. Most weathered units in the highs of paleo-structure have been eroded with poor continuity. Bedrock reservoirs are mainly developed in semi-weathered units. Of oil-producing intervals, 75% are within 20 m from the top of the bedrocks in the study area, and 25% of oil-producing intervals are developed at the positions at about 20–50 m from the top. Neither oil not gas is discovered in fresh bedrocks. FMI data suggests that induced fractures in bedrocks are near N-S direction, while borehole collapse is near E-W direction.

Three fracture types were developed in semi-weathered granite, e.g., structural fractures, dissolution fractures, and weathering

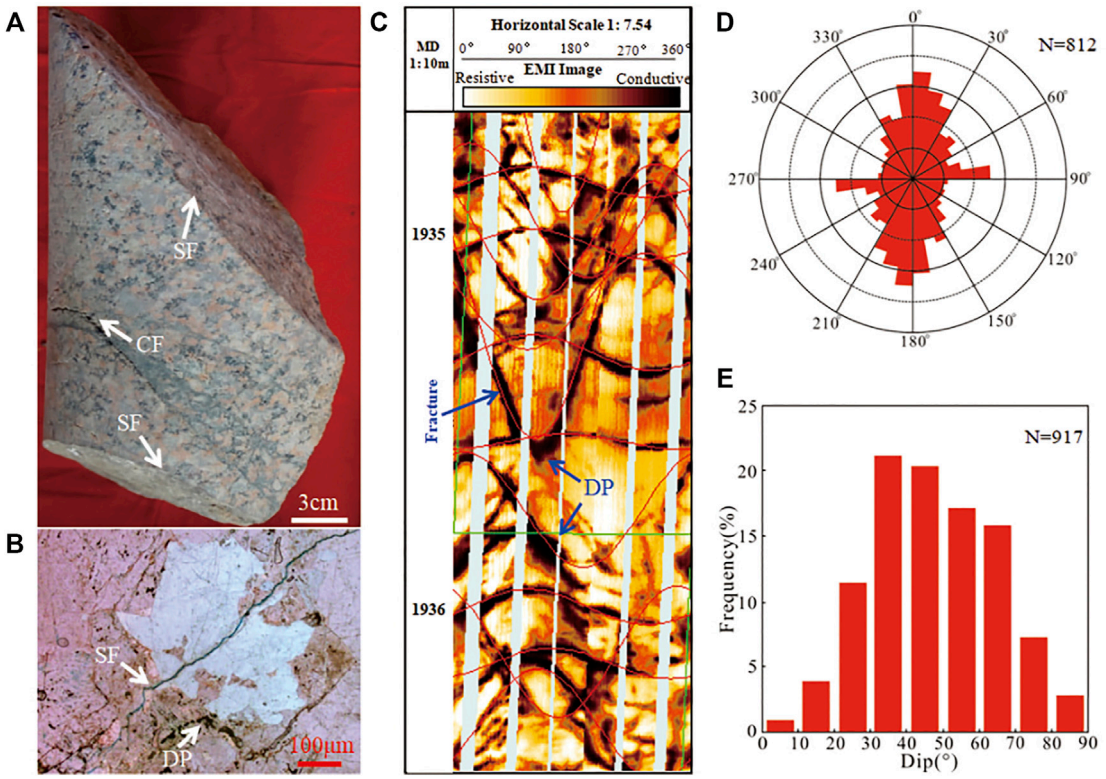

FIGURE 4 | Fracture development on cores and FMI image. **(A)** A group of fractures in granite. Well W2: depth 2,104.2 m. SF is shear fracture, CF is corrosion fracture. **(B)**Thin section showing shear fracture in granite. Well W18: depth 2,128.3 m. DP is dissolution pore.**(C)** Network fractures in FMI image of Well W5. **(D)** Rose diagrams of natural fracture strike in granite from FMI. **(E)** Dip angles of natural fracture in granite from FMI and cores. See **Figure 1** for wells location.

fractures. Structural fractures were derived from local tectonic events or regional tectonic stress fields (Chad et al., 2003). Shear fractures related to faults are popular in granite, accounting for over 90%. About 72.5% of near E-W extending shear fractures, occurring mainly from the Late Hercynian to Indosinian, are filled with quartz, which are ineffective, while only 16.7% of N-S extending shear fractures, occurring mainly during the Himalayan, is filled. These fractures have straight and smooth surfaces and large cutting. Dissolution along structural fractures is common, creating dissolution fractures and dissolution pores (**Figures 4A,B**). Fracture networks can be identified from FMI images with obvious dissolution (**Figure 4C**). Weathering fractures are irregularly distributed at the top of semi-weathered bedrock, with small-scale and poor connectivity. Effective fractures in granite are 4.2/m in average line density, and are about 20–50 μm in aperture with average value of 33.2 μm. Fracture porosity is generally lower than 0.1%, with the peak at 0.01–0.04%, while average fracture permeability is 35.3×10^{-3} μm^2, e.g., average permeability of near N-S trending and near E-W trending fractures is 40.7×10^{-3} μm^2 and 9.4×10^{-3} μm^2, respectively. These effective fractures assume chiefly the near N-S strike (**Figure 4D**), while primary seepage orientation at some wells (e.g., W21 well and W22 well) is along NNE-SSW direction.

Structural fractures, diagenetic fractures, and a small amount of dissolution fractures can be observed in slates in the semi-weathered unit. Three stages of fractures can be identified based on fracture distribution (**Figure 5A**). Diagenetic fractures and structural fractures near the top of semi-weathered units are mostly filled by shale or quartz, while the density of filled structural fractures decreases gradually with increasing burial depth. Although dissolution pores and dissolution fractures are also found in slate (**Figure 5B**), dissolution in slate is weak compared with granite. The fracture porosity is generally lower than 0.05%, with the peak at 0.01–0.02%, and the average fracture permeability is 21.4×10^{-3}μm^2 in near NNE-SSW strike. The effective fractures have average linear density of 2.6/m, which assume chiefly the near NNE-SSW strike (**Figure 5C**) with dip angle of 30–70° (**Figure 5D**).

DISCUSSION

A large number of natural fractures have been developed in the bedrocks in the study area due to multi-stage tectonic movements (Jun et al., 2016; Wu et al., 2018; Sun et al., 2018), e.g., Indosinian movement, Yanshan movement, and Himalayan movement. NW-SE compressive stress during Late Hercynian to Indosinian (Peng et al., 2015) resulted in near E-W trending structural fractures. The bedrocks were uplifted and weathered during Indosinian to Yanshanian (Wang et al., 2020), creating

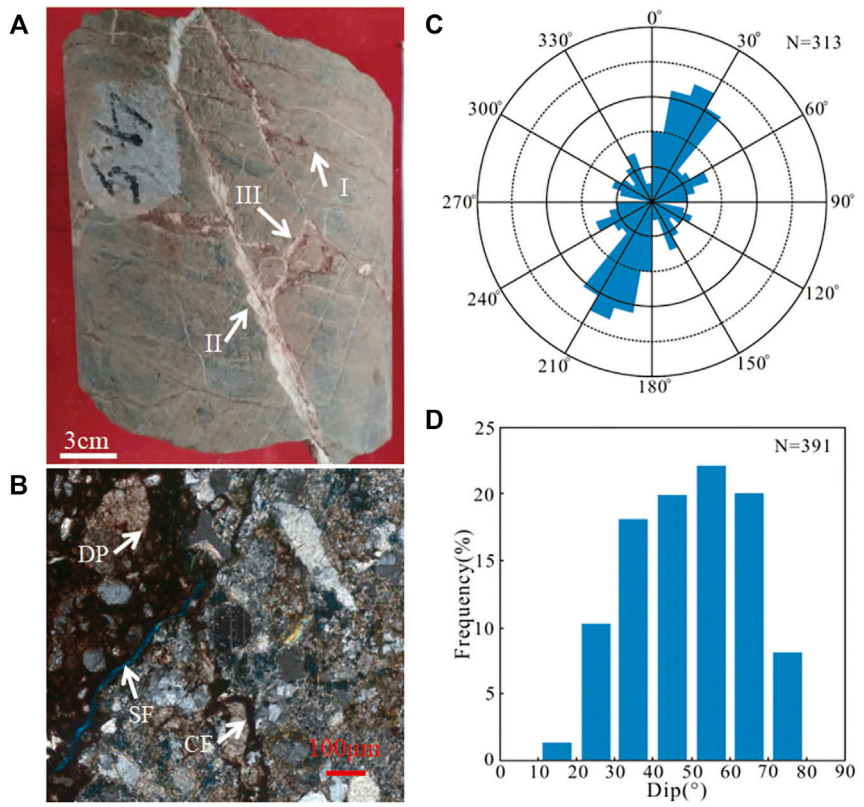

FIGURE 5 | Fracture characteristics in slate.**(A)** Fractures are completely filled with minerals in the weathered layer. Well W18: depth 1847.6 m.**(B)**Shear fracture observed from thin sections. Well W2: depth 1848.4 m. **(C)** Rose diagrams of natural fracture strike in slate from FMI. **(D)** Dip angles of natural fracture in slate from FMI data and cores. See **Figure 1** for wells location.

dissolution pores and fractures. NNE-SSW compressive stress, Kunbei fault, and piedmont fault in the Himalayan worked together to create considerable secondary faults and near N-S structural fractures in the study area (Wang and Peng, 1991). However, no effective fracture occurred in the weathered unit at the top of the bedrocks. The semi-weathered unit can be a high-quality reservoir because of dissolution pores and fractures (including dissolution fractures). The fracture intensity varies greatly with tectonic stress (Zeng et al., 2016), while difference in rock mechanical properties can result in varied fracture density under the same tectonic stress. Also, gravity is an important factor controlling the stress state of rocks (Narr and Suppe., 1991). Generally, fracture density decreases with increasing depth due to increasing rock compressive strength (**Figure 6A**). Furthermore, faults are important factors controlling fracture intensity and distribution in the study area, e.g., fault activity can produce stress disturbance, resulting in high fracture density near faults (Laubach et al., 2018). Therefore, fracture density decreases with lateral distance between fracture and fault plane (**Figure 6B**).

Effective fractures are critical for seepage behaviors of reservoirs, which is determined by fracture density, fracture aperture, dip angle, and fracture scale (Nelson et al., 2000; Wang Z. S. et al., 2021). Induced fractures are commonly parallel to the present-day maximum horizontal *in-situ* stress, while borehole collapse is perpendicular to the present-day maximum horizontal *in-situ* stress (Barton et al., 1988; Scelsi et al., 2019). Effective fractures in granite and slate in the study area have high density near N-S and NNE-SSW directions, respectively (**Figure 4D**), which is parallel to or intersected at a small angle with the present day maximum horizontal *in-situ* stress direction. Also, fractures in granite and slate have large apertures near N-S and NNE-SSW directions under the present day *in-situ* stress, respectively. Fractures in different directions share similar dip angles, ranging from 30° to 70°(**Figure 4E** and **Figure 5D**). Consequently, dominant seepage channels in granite and slate are generally developed near N-S and NNE-SSW directions, respectively, which varies slightly in different positions.

The basement faults and unconformities are primary oil and gas migration channels for bedrock reservoirs in Kunbei fault terrace belt (Cao et al., 2013). Fractures (including dissolution fractures) and dissolution pores are connected with each other to form conduit networks, contributing to lateral oil and gas migration along unconformities (Cukur et al., 2010). Dissolution fractures and pores provide favorable storage space in bedrock reservoirs, while dissolution fractures are also main seepage channels. They were developed due to the dissolution of soluble mineral along early effective fractures (Alhuraishawy et al., 2018), which depended on

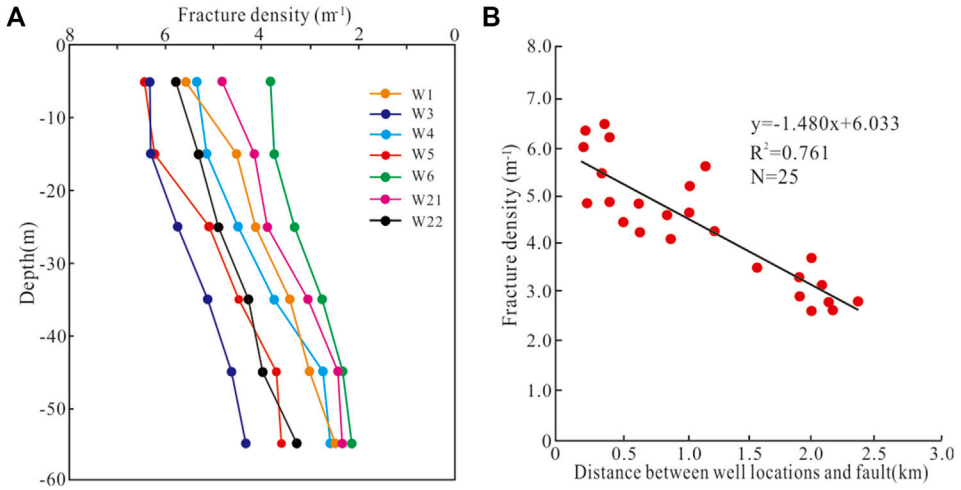

FIGURE 6 | Distribution characteristics of bedrock fractures. (A)Fracture density varies with depth (data from FMI, and the point 0 is at the top of semi-weathered unit). (B) Relationship between fracture density and distance between well points and fault (data from FMI and cores).

soluble mineral contents in bedrocks and their contact with formation water (Hakala et al., 2021). Since sericitization or kaolinization easily occurs to feldspar particles in granite and vermiculization can occur to biotite, the dissolution prevails in granite compared with slate and decreases with increasing depth. Fault zone and semi-weathered unit in Kunbei fault terrace belt have high fracture density and intensive dissolution, which is favorable for oil and gas accumulation. Effective fractures control the formation and distribution of dissolution fractures and pores in the later stage as well as dominant seepage direction, which is one of the key factors controlling oil and gas accumulation and reservoir development in bedrocks.

CONCLUSION

A large number of natural fractures with different types have been developed in the bedrocks in the study area due to diagenesis and multi-stage tectonic movements, e.g., Indosinian movement, Yanshan movement, and Himalayan movement. Pores and fractures are poorly developed in weathered units at the top of bedrocks in the Kunbei fault terrace belt, which are not effective reservoirs. Formation water migration along early effective fractures can create dissolution fractures and pores in the semi-weathered unit, acting as primary storage space for oil and gas. Fracture intensity varies greatly with lithology, e.g., dissolution fractures are well developed in granite. The fracture density is closely related to tectonic stress and other factors, e.g., lithology, burial depth, and structural location. Effective fractures control the distribution of dissolution fractures and pores developing in later stage as well as dominant seepage direction, which is critical for oil and gas accumulation and reservoir development in bedrocks. Oil and gas accumulation could be well developed in bedrock reservoirs near fault zones and semi-weathered units in the Kunbei fault terrace belt.

DATA AVAILABILITY STATEMENT

The original contributions presented in the study are included in the article/Supplementary Material, further inquiries can be directed to the corresponding author.

AUTHOR CONTRIBUTIONS

ZW: Methodology, Writing—Original Draft; HX: Investigation, Conceptualization; LW: Experiment; LX: Resources, Software; ZZ: Visualization, Data Curation; LG: Funding acquisition; ZY: Resources, Methodology; FL: Data Curation.

FUNDING

This study is financially supported by the National Natural Science Foundation of China (No: 41172015).

ACKNOWLEDGMENTS

The authors wish to thank Bing Hou, professor at China University of Petroleum (Beijing), for his sincere and generous help.

REFERENCES

Alhuraishawy, A. K., Bai, B., Wei, M., Geng, J., and Pu, J. (2018). Mineral Dissolution and fine Migration Effect on Oil Recovery Factor by Low-Salinity Water Flooding in Low-Permeability sandstone Reservoir. *Fuel* 220, 898–907. doi:10.1016/j.fuel.2018.02.016

Bagriy, I. D., and Griga, M. Y. (2015). Main Features of Prediction the Hydrocarbon Accumulation of Sedimentary and Basement Rocks on Impact Structures with Stagr Technology. *Geol. J.* 350 (1), 107–114. doi:10.30836/igs.1025-6814.2015.1.139103

Barton, C. A., Zoback, M. D., and Burns, K. L. (1988). *In-Situ* Stress Orientation and Magnitude at the Fenton Geothermal Site, New Mexico, Determined from Wellbore Breakouts. *Geophys. Res. Lett.* 15 (5), 467–470. doi:10.1029/GL015i005p00467

Cao, Z. L., Wei, Z. F., Zhang, X. J., Yan, C. F., Tian, G. R., and Ma, F. (2013). Oil-gas Source Correlation in Dongping Area, Qaidam Basin. *Lithologic Reservoirs* 25 (3), 17–21. (in Chinese with English abstract).

Chad, A. U., Michele, L. C., Simo, J. A., and Muldoon, M. A. (2003). Stratigraphic Controls on Vertical Fracture Patterns in Silarian Dolomite, Northeastern Wisconsin. *AAPG Bull.* 87, 121–142. doi:10.1109/PES.2003.1271067

Chen, G. M., Wan, Y., Zhang, P. P., Xia, M. Q., and Zhang, D. W. (2010). Traps Characteristics in north Kunlun Faults of Qaidam basin. *J. Southwest Pet. Univ. (Science & Technology Edition)* 32 (4), 39–44. (in Chinese with English abstract).

Chen, S. J., Lu, J. G., Ma, D. D., Wang, L. Q., Zhao, M. J., Xue, J. Q., et al. (2012). Origin and Accumulation Characteristics of the Oil from Hanging walls of Kunbei Fault-Terrace belt in Qaidam Basin. *Acta Petrolei Sinica* 33 (6), 915–924. (in Chinese with English abstract).

Cukur, D., Horozal, S., Kim, D. C., Lee, G. H., Han, H. C., and Kang, M. H. (2010). The Distribution and Characteristics of the Igneous Complexes in the Northern east china Sea Shelf basin and Their Implications for Hydrocarbon Potential. *Mar. Geophys. Res.* 31 (4), 299–313. doi:10.1007/s11001-010-9112-y

Dühnforth, M., Anderson, R. S., Ward, D., and Stock, G. M. (2010). Bedrock Fracture Control of Glacial Erosion Processes and Rates. *Geology* 38 (5), 423–426. doi:10.1130/G30576.1

Fu, S. T., Xu, L. G., and Gong, Q. L. (2010). Hydrocarbon Geologic Characteristics and Suggestions for Further Exploration and Research in the Southwestern Qaidam basin. *China Pet. Exploration* 15 (1), 6–10. (in Chinese with English abstract).

Gao, X. Z., Sun, L., Wang, L. Q., Cai, M. L., Zhang, G. Q., and Jiang, Z. L. (2014). Migration of Petroleum in Kunbei Faulted Terrace of Qaidam Basin. *Acta Geoscientica Sinica* 35 (1), 93–100. (in Chinese with English abstract).

Hakala, J. A., Paukert Vankeuren, A. N., Scheuermann, P. P., Lopano, C., and Guthrie, G. D. (2021). Predicting the Potential for mineral Scale Precipitation in Unconventional Reservoirs Due to Fluid-Rock and Fluid Mixing Geochemical Reactions. *Fuel* 284, 118883. doi:10.1016/j.fuel.2020.118883

Hoffman, B. T., and Narr, W. (2012). Using Production Logs (PLT) to Estimate the Size of Fracture Networks. *J. Pet. Sci. Eng.* 98-99, 11–18. doi:10.1016/j.petrol.2012.08.019

Huang, J. X., Peng, S. M., and Wang, X. J. (2006). Applications of Imaging Logging Data in the Research of Fracture and Ground Stress. *Acta Petrolei Sinica* 27 (6), 65–69. (in Chinese with English abstract).

Jan, S. R., Lauritsen, T., and Mauring, E. (1995). Locating Bedrock Fractures beneath Alluvium Using Various Geophysical Methods. *J. Appl. Geophys.* 34 (2), 158. doi:10.1016/0926-9851(96)80894-9

Jun, Y. J., Zhang, X. L., Zhang, Y. S., and Chen, Y. (2016). Fracture Characteristics of Bedrock Reservoir in the North-Kunlun Faults Zone, Qaidam Basin. *J. Jilin Univ. (Earth Sci. Edition)* 46 (6), 1660–1671. doi:10.13278/j.cnki.jjuese.201606106

Laubach, S. E., Lamarche, J., Gauthier, B. D. M., Dunne, W. M., and Sanderson, D. J. (2018). Spatial Arrangement of Faults and Opening-Mode Fractures. *J. Struct. Geology.* 108, 2–15. doi:10.1016/j.jsg.2017.08.008

Li, J. M., Shi, L. L., Wang, L. Q., and Wu, G. D. (2011). Characteristics of Basement Reservoir in Kunbei Fault Terrace belt in Southwestern Qaidam Basin. *Lithologic Reservoirs* 23 (2), 20–23. (in Chinese with English abstract).

Lianbo, Z., and Xiang-Yang, L. (2009). Fractures in sandstone Reservoirs with Ultra-low Permeability: A Case Study of the Upper Triassic Yanchang Formation in the Ordos Basin, China. *Bulletin* 93 (4), 461–477. doi:10.1306/09240808047

Liu, G. Z., Zhang, D. S., and Li, N. W. (2015). Characteristics of Basement Reservoirs and Hydrocarbon Accumulation Conditions in the Northern Kunlun Fault Zone. *Lithologic Reservoirs* 27 (2), 62–69. (in Chinese with English abstract).

Liu, H. T., Ma, L. X., Wang, Z. Y., and Sun, D. Q. (2008). Study on Dynamic Evolution of Petroleum System in the Western Qaidam Basin. *Acta Petrolei Sinica* 29 (1), 16–22.

Liu, Z. (2012). New Progress and Prospects in the Study of Rock-Weathering-Related Carbon Sinks. *Chin. Sci. Bull.* 57 (2-3), 95–102. doi:10.1360/972011-1640

Luthi, S. M., and Souhaité, P. (1990). Fracture Apertures from Electrical Borehole Scans. *Geophysics* 55, 821–833. doi:10.1190/1.1442896

Ma, L., Liu, Q. X., and Zhang, J. L. (2006). A Discussion of Exploration Potentials of Basement Hydrocarbon Reservoir. *Nat. Gas Industry* 26 (1), 8–11. (in Chinese with English abstract).

Narr, W., and Suppe, J. (1991). Joint Spacing in Sedimentary Rocks. *J. Struct. Geology.* 13, 1037–1048. doi:10.1016/0191-8141(91)90055-N

Niu, H. L., Hu, X., Xu, Z. Q., Wang, L., and Liu, Y. B. (2010). Evaluation of Imaging Logging and Fracture Prediction in Fractured Basement Reservoirs. *Acta Petrolei Sinica* 31 (2), 264–269. (in Chinese with English abstract).

Peng, Y., Ma, Y. S., Liu, C. L., Sun, J. P., Cheng, H. Y., Dai, K., et al. (2015). An Analysis of Late Hercynian-Indosinian Paleotectonic Stress on the Northern Margin of the Qaidam Basin. *Acta Geoscientica Sinica* 36 (1), 51–59. doi:10.3975/cagsb.2015.01.06

Qu, H. Z., Zhang, F. X., Wang, Z. Y., Yang, X. T., Liu, H. T., Ba, D., et al. (2016). Quantitative Fracture Evaluation Method Based on Core-Image Logging: A Case Study of Cretaceous Bashijiqike Formation in Ks2 Well Area, Kuqa Depression. *Tarim Basin, NW China: Pet. Exploration Development* 43, 425–433. (in Chinese)(in Chinese with English abstract). doi:10.1016/s1876-3804(16)30054-4

R. A. Nelson,1 E. P. Mold, R. A., Moldovany, E. P., and Matcek, C. C. (2000). Production Characteristics of the Fractured Reservoirs of the La Paz Field, Maracaibo basin, Venezuela. *Bulletin* 84, 1791–1809. doi:10.1306/8626C393-173B-11D7-8645000102C1865D

Scelsi, G., De Bellis, M. L., Pandolfi, A., Musso, G., and Della Vecchia, G. (2019). A Step-by-step Analytical Procedure to Estimate the *In-Situ* Stress State from Borehole Data. *J. Pet. Sci. Eng.* 176, 994–1007. doi:10.1016/j.petrol.2019.01.100

Shanley, K. W., and Cluff, R. M. (2015). The Evolution of Pore-Scale Fluid-Saturation in Low-Permeability sandstone Reservoirs. *Bulletin* 99, 1957–1990. doi:10.1306/03041411168

Sun, X. J., Yang, W., Bai, Y. D., Xie, Mei., and Shi, Z. H. (2018). Bedrock Reservoir Characterization and Favorable Zones in Qaidam Basin. *Spec. Oil Gas Reservoirs* 25 (6), 49–54. doi:10.3969/j.issn.1006-6535.2018.06.009

Tamagawa, T., and Pollard, D. D. (2008). Fracture Permeability Created by Perturbed Stress fields Around Active Faults in a Fractured Basement Reservoir. *Bulletin* 92 (6), 743–764. doi:10.1306/02050807013

Tong, K., Li, B., Dai, W., Zheng, H., Zhang, Z., Cheng, Q., et al. (2017). Sparse Well Pattern and High-Efficient Development of Metamorphic Buried hills Reservoirs in Bohai Sea Area, china. *Pet. Exploration Development* 44 (4), 625–635. doi:10.1016/s1876-3804(17)30071-x

Wang, J. Q., Liang, J., Chen, J. W., Zhang, Y. G., Zhao, Q. F., Dong, H. P., et al. (2021a). Characteristics of the Recently Bedrock Hydrocarbon Reservoir in China Seas and Future Exploration Directions. *Mar. Geology. Quat. Geology.* 41 (6), 151–162. doi:10.16562/j.cnki.0256-1492.2021031201

Wang, J. R., and Peng, Z. L. (1991). The Tectonic Stress Field for the Qaidam Basin and its Geological Significance. *J. Lanzhou Univesity (Natural Sciences)* 27 (3), 120–125. doi:10.13885/j.issn.0455-2059.1991.03.020

Wang, L. L., Yu, D. D., Fu, Y., and Yan, M. (2020). Tectonic Evolution and Differential Deformation Controls on Oilfield Water Distribution in Western Qaidam Basin. *Pet. Geology. & Exp.* 42 (2), 186–192. doi:10.11781/sysydz202002186

Wang, Z. S., Meiri, M., Xu, D. H., Fang, J. C., Li, J., Liu, D. J., et al. (2021b). Seepage Behavior of Fractures in Paleogene Sandstone Reservoirs in Nanpu Sag,

Bohai Bay Basin, Eastern China. *Front. Earth Sci.* 9, 1–10. doi:10.3389/feart.2021.718733

Wishart, D. N., Slater, L. D., and Gates, A. E. (2008). Fracture Anisotropy Characterization in Crystalline Bedrock Using Field-Scale Azimuthal Self Potential Gradient. *J. Hydrol.* 358 (1-2), 35–45. doi:10.1016/j.jhydrol.2008.05.017

Wu, G., Li, H., Zhang, L., Wang, C., and Zhou, B. (2012). Reservoir-forming Conditions of Ordovician Weathering Crust in the Maigaiti Slope, Tarim basin, NW china. *Pet. Exploration Development* 39 (2), 155–164. doi:10.1016/S1876-3804(12)60028-7

Wu, J., Gao, X. Z., Zhou, W., Zhang, Y. S., Yang, Y., and You, C. (2018). Base Rock Weathering Crusts and Petroleum Accumulation in Dongping Area, Qaidam Basin. *Xinjiang Pet. Geology*. 39 (6), 666–672. doi:10.7657/XJPG20180606

Wu, Y. X., Ma, D., Liu, J. L., Xue, J. Q., Zhang, N., Liu, H. Z., et al. (2014). Geological Conditions of Basement Oil Pools in Western Qaidam Basin. *Nat. Gas Geosci.* 25 (11), 1689–1696. (in Chinese with English abstract).

Zeng, L., Jiang, J., and Yang, Y. (2010). Fractures in the Low Porosity and Ultra-low Permeability Glutenite Reservoirs: A Case Study of the Late Eocene Hetaoyuan Formation in the Anpeng Oilfield, Nanxiang Basin, China. *Mar. Pet. Geology*. 27, 1642–1650. doi:10.1016/j.marpetgeo.2010.03.009

Zeng, L., Lyu, W., Li, J., Zhu, L., Weng, J., Yue, F., et al. (2016). Natural Fractures and Their Influence on Shale Gas Enrichment in Sichuan Basin, China. *J. Nat. Gas Sci. Eng.* 30, 1–9. doi:10.1016/j.jngse.2015.11.048

Zhang, Y., Zeng, L., Lyu, W., Sun, D., Chen, S., Guan, C., et al. (2021). Natural Fractures in Tight Gas Sandstones: a Case Study of the Upper Triassic Xujiahe Formation in Xinchang Gas Field, Western Sichuan basin, China. *Geol. Mag.* 158 (9), 1543–1560. doi:10.1017/S001675682100008X

Zhu, M.., Liu, H.., Liang, S., and Zhangg, P. (2020). Structural Division of Granite Weathering Crusts and Effective Reservoir Evaluation in the Western Segment of the Northern belt of Dongying Sag, Bohai Bay Basin, NE Chinat. *Mar. Pet. Geology*. 121 (2), 104612. doi:10.1016/j.marpetgeo.2020.104612

Conflict of Interest: ZW was employed by the Company College of Mining Engineering, Liaoning Technical University.

Author ZW is employed by College of Mining Engineering, Liaoning Technical University, China. Author HX is employed by Zhundong Oil Production Plant, Xinjiang Oilfield Company of PetroChina, China. Author LW is employed by Research Institute of Petroleum Exploration and Development of PetroChina, China. Author LX is employed by Research Institute of Petroleum Exploration and Development of Qinghai Oilfield Company, PetroChina, China. The remaining authors declare that the research was conducted in the absence of any commercial or financial relationships that could be construed as a potential conflict of interest.

HX was employed by the Company Xinjiang Oilfield Company of Petro China.

LW was employed by the Company Research Institute of Petroleum Exploration and Development of Petro China.

LX was employed by the Company Research Institute of Petroleum Exploration and Development of Qinghai Oilfield Company, Petro China.

The remaining authors declare that the research was conducted in the absence of any commercial or financial relationships that could be construed as a potential conflict of interest.

Publisher's Note: All claims expressed in this article are solely those of the authors and do not necessarily represent those of their affiliated organizations, or those of the publisher, the editors and the reviewers. Any product that may be evaluated in this article, or claim that may be made by its manufacturer, is not guaranteed or endorsed by the publisher.

Copyright © 2022 Wang, Xiang, Wang, Xie, Zhang, Gao, Yan and Li. This is an open-access article distributed under the terms of the Creative Commons Attribution License (CC BY). The use, distribution or reproduction in other forums is permitted, provided the original author(s) and the copyright owner(s) are credited and that the original publication in this journal is cited, in accordance with accepted academic practice. No use, distribution or reproduction is permitted which does not comply with these terms.